Computers and Concrete, *Vol. 24, No. 1 (2019) 63-71*
DOI: https://doi.org/10.12989/cac.2019.24.1.063

Residual properties of high-strength fiber reinforced concrete after exposure to high temperatures

Chao-Wei Tang*[1,2,3]

[1]*Department of Civil Engineering & Geomatics, Cheng Shiu University, No. 840, Chengching Rd., Niaosong District, Kaohsiung City, Taiwan R.O.C.*
[2]*Center for Environmental Toxin and Emerging-Contaminant Research, Cheng Shiu University, No. 840, Chengching Rd., Niaosong District, Kaohsiung 83347, Taiwan*
[3]*Super Micro Mass Research & Technology Center, Cheng Shiu University, No. 840, Chengching Rd., Niaosong District, Kaohsiung 83347, Taiwan*

(Received January 16, 2019, Revised May 1, 2019, Accepted June 4, 2019)

Abstract. Thermal energy from high temperatures can cause concrete damage, including mechanical and chemical degradation. In view of this, the residual mechanical properties of high-strength fiber reinforced concrete with a design strength of 75 MPa exposed to 400-800℃ were investigated in this study. The test results show that the average residual compressive strength of high-strength fiber reinforced concrete after being exposed to 400-800℃ was 88%, 69%, and 23% of room-temperature strength, respectively. In addition, the benefit of steel fibers on the residual compressive strength of concrete was limited, but polypropylene fibers can help to maintain the residual compressive strength and flexural strength of concrete after exposure to 400-600℃. Further, the load-deflection curve of specimen containing steel fibers exposed to 400-800℃ had a better fracture toughness.

Keywords: fiber reinforced concrete; residual mechanical properties

1. Introduction

Concrete is a cement-based composite material, which has become one of the most widely used building materials in the world due to its relatively low price and many advantages (Somayaji 2001). As a structural composite, the cement matrix in concrete consists of the combination of two or more non-miscible phases to form a macroscopically homogeneous material, which is essentially a heterogeneous brittle composite material (Bastos *et al*. 2016). As a result, concrete is relatively brittle, and its tensile strength is typically only about one-tenth of its compressive strength (Mehta and Monteiro 2006). In order to increase the energy absorption capacity and toughness of concrete, fibers of various shapes and sizes made of steel, plastic, glass and natural materials have been blended into the cement matrix to form so-called fiber reinforced concrete (FRC) (Xiong and Richard Liew 2015, Xu *et al*. 2016, Kim *et al*. 2016, Lee and Yi 2016, Nematzadeh and Poorhosein 2017, Saleem 2017, Zhang *et al*. 2018). Fibers can inhibit crack initiation, thereby reducing the source and size of cracks. In the stress process, the fiber not only inhibits the extension and expansion of cracks in the matrix, but also alleviates the stress concentration at the crack tip, so that the concrete’s tensile strength, deformation ability, and resistance to dynamic load capacity are significantly improved.

Based on compressive strength, concrete can be divided into four major categories: low-strength concrete (less than 20 MPa), medium-strength concrete (20-40 MPa), high-strength concrete (more than 40 MPa), and ultra-high-strength concrete exceeding 150 MPa (Larrard and Sedran 2002). The use of high-strength concrete (HSC) has many advantages such as greatly reducing the size of structural concrete components and effectively increasing the available space of structures, and thus its application has been increasing in construction projects. However, high temperatures and fires can cause damage to HSC, including mechanical degradation and chemical degradation. Among them, mechanical degradation is mainly caused by thermal strain incompatibility and excessive pore pressure. As for chemical degradation, it mainly occurs in the form of dehydration, dihydroxylation, and decomposition of calcium silicate hydrates and other products of cement hydration (Way and Wille 2016). Once mechanical degradation has combined with chemical degradation, premature failure of the concrete accelerates, which in turn leads to failure of reinforced high-strength concrete structures. Therefore, fire damage is a special failure mode of reinforced high-strength concrete structures, which has a great impact on the overall safety of the structure and is of great significance and value.

With the increase of the application of HSC, the research of its fire resistance has been paid more and more attention. In particular, HSC has been found to be susceptible to explosive spalling in an environment with rapidly rising temperatures. The spalling is mainly caused by thermal stress due to the temperature gradient during heating (Sanjayan and Stocks 1993, Chan *et al*. 2000, Ko *et*

∗Corresponding author, Professor
E-mail: tangcw@gcloud.csu.edu.tw

ISSN: 1598-8198 (Print), 1598-818X (Online)

Table 1 Planning of experimental variables

Group	Mix No.	f_c'	Fiber content (Volume %)	Targeted temperature (℃)
Control group	N75	75 MPa	0	400, 600, and 800
Experimental group	F75-S	75 MPa	SF (1%)	400, 600, and 800
	F75-P	75 MPa	PP (0.1%)	400, 600, and 800
	F75-M	75 MPa	SF (1%)+PP (0.1%)	400, 600, and 800

Notes: f_c'=specified concrete strength; SF=steel fiber; PP=Polypropylene fiber.

Table 2 Physical properties of coarse/fine aggregate

Aggregate type	γ_d (SSD)	W_a (SSD) (%)	U_w (dry-rodded) (kg/m^3)	FM
Fine aggregate	2.60	1.25	-	2.70
Coarse aggregate	2.63	1.17	1532	-

Notes: γ_d=specific weight; W_a=water absorption; SSD=saturated surface dry condition; U_w=unit weight; FM=fineness modulus.

Table 3 Mix proportions of concrete

Group	Mix No.	Cement (kg/m^3)	Slag (kg/m^3)	Water (kg/m^3)	Aggregate (kg/m^3) FA	Aggregate (kg/m^3) CA	SP (kg/m^3)	Steel fiber (kg/m^3)	PP (kg/m^3)
Control group	N75	386	128	180	645	1020	3.375	-	-
Experimental group	F75-S	386	112	180	645	1020	3.375	78	0
	F75-P	386	112	180	645	1020	3.375	0	0.9
	F75-M	386	112	180	645	1020	3.375	78	0.9

Note: F=fiber concrete; N=ordinary concrete; digits=strength level; FA=fine aggregate; CA=coarse aggregate; SP=superplasticizer; PP=polypropylene fiber.

al. 2011). In view of this, many researchers have been engaged in exploring the spalling behavior of HSC at high temperatures. For instance, Varona *et al*. (2018) investigated the mechanical properties of hybrid fiber reinforced normal- and high-strength concrete after exposure to high temperatures. Their test results clearly showed that the effect of high temperature on the residual mechanical properties of hybrid fiber reinforced concretes was not as severe as that of steel fiber reinforced concrete found in previous references. In addition, it is worth mentioning that polypropylene fibers can mitigate or prevent the explosive spalling (Poon *et al*. 2004, Siddique and Kaur 2012, Ding *et al*. 2012, Ozawa and Morimoto 2014, Yan *et al*. 2015). This is mainly because the polypropylene fibers melt after the temperature inside concrete reaches approximately 170 ℃, which produces microchannels for the release of the vapor pressure in the concrete. As a result, the amount of heat absorbed is less for dehydration of chemically bound water (Bilodeau *et al*. 2004, Kodur 2014, Xiong and Richard Liew 2015). In addition, some experimental studies show that polypropylene fiber can improve the relative residual compressive strength of concrete composites after a fire (Qadi and Sleiman 2014, Serrano *et al*. 2016). However, the effect of polypropylene fibers on the mechanical degradation of various strength HSCs is a function of temperature. Some experimental studies have pointed out that polypropylene fibers have a negative effect on the residual mechanical properties of concrete after high-temperature exposure because they significantly reduce the residual compressive strength, elastic modulus, and tensile strength as well as they increase the peak strain (Sideris *et al*. 2009, Sideris and Manita 2013, Khaliq and Kodur 2011). In summary, the effect of polypropylene fiber on the mechanical degradation of concrete is not fully understood and remains to be further explored (Chan *et al*. 2000, Poon *et al*. 2004).

In view of the above considerations, the residual mechanical properties of high-strength fiber reinforced concrete with a design strength of 75 MPa exposed to 400-800℃ were investigated in this study.

2. Experimental procedure

2.1 Experimental program

In this study, the test variables include concrete types (control group: ordinary concrete; experimental group: fiber reinforced concrete), fiber types (steel fiber and polypropylene fiber), and fire temperature (400, 600, and 800℃). The planned variation of the experimental variables is shown in Table 1.

2.2 Materials

Materials used for making specimens included cement, slag, fine and coarse aggregates, fiber, and superplasticizer. Local ordinary Portland cement (OPC) with a specific gravity of 3.15 and a fineness of 3400 cm^2/g in accordance with ASTM C150/C150M (ASTM C150/C150M-15 2015) was used throughout the research work. Locally available slag with a specific gravity of 2.9 and a fineness of 6000 cm^2/g was used. Fine and coarse aggregates were selected in accordance with ASTM C33/C33M (ASTM C33/C33M-13 2013). The fine aggregate was obtained from a local river, and the coarse aggregate was continuous grading crushed stone with a maximum particle size of 19 mm. The specific weight, water absorption, and unit weight of these aggregates are shown in Table 2. Local steel fibers with a density of 1.78 g/cm^3 and polypropylene fibers with a melting point of 160℃ to 170℃ and a density of 0.9 g/cm^3 were used. In order to ensure the good workability of the prepared concrete, a superplasticizer, Sikament-1250 produced by Sika Taiwan Co., Ltd., was used.

2.3 Mix proportions

The 28-day design compressive strength of high-strength concrete was 75 MPa. Some trial mixtures were prepared to obtain the target strength at 28 days of age, along with proper workability of 90 to 200 mm. The mix proportions for the FC and the NC are given in Table 3. The

Fig. 1 Compressive strength test configuration

Fig. 2 Flexural strength test configuration

abbreviations for identifying each concrete indicate the type of concrete -fiber concrete (F) or ordinary concrete (N), the strength of concrete (75 MPa), and the type of fiber (S: steel fiber, P: polypropylene fiber, M: hybrid fiber). Prior to mixing, the aggregates were cured indoors until the required saturated surface-dry condition was reached. In mixing, the cement, slag, fiber, and fine and coarse aggregates were first uniformly mixed. Thereafter water and superplasticizer were slowly added and mixing was continued until the uniform mix was obtained. After the concrete was mixed, its fresh properties were first measured and recorded.

2.4 Fabrication of specimens

Concrete specimens for each test were cast out of each mixture and compacted using an external vibrator. Along with each mixture, twelve 100 mm in diameter×200 mm in height cylindrical specimens were cast for compressive strength test and elastic modulus test; twelve prism specimens (3600 mm in length×100 mm in width×100 mm in thickness) were cast for flexural strength of concrete. After casting, all the specimens were covered overnight with a wet hessian and polyethylene sheets for a period of 24 hours. The specimens were then demolded after 24 hours. Following demolding, all the specimens were placed in a water bath in the laboratory. After curing, the specimens were removed from the water bath one day before the test.

2.5 Testing methods and instrumentation

According to the ASTM C39 standard test method, cylindrical specimens were used to test at 28 days of age (Fig. 1). As for the flexural strength, it is based on ASTM C78 standard test method for concrete flexural strength (Fig. 2). The elastic modulus of concrete was tested in accordance with ASTM C469 using cylindrical specimens at 28 days of age. On the other hands, the specimens were heated at a prescribed rate (10℃/min.) until the temperature inside the furnace reached the target temperatures. After achieving the targeted maximum temperature, the furnace temperature was maintained for 60 minutes to achieve a better thermal steady state in the whole specimen. The furnace power switch was turned off immediately, and the specimens were cooled to room temperature by opening the furnace door before the residual strength tests were carried out.

Table 4 Results of slump and unit weight of concrete

Group	Mix No.	Slump (cm)	Unit weight (kg/m^3)
Control group	N75	21	2259
Experimental group	F75-S	20	2338
	F75-P	9	2270
	F75-M	9	2347

3. Experimental results and discussion

3.1 Fresh properties of concrete

The result of the fresh properties of each concrete mixture was listed in Table 4. As can be seen from the table, the slump value ranged from 9 to 21 cm. The N75 mix of the control group had a slump of 21 cm, indicating that it had very good workability. As for the experimental group, the F75-S mix with steel fiber had a slump of 20 cm, but the slump of both the F75-P and F75-M mixes with polypropylene fiber was only 9 cm. The reason is that the polypropylene fibers are very fine (about 50000-300 million strands per kilogram), resulting in a stiffer mixture and leading to reduced workability. Moreover, Table 4 shows that the unit weight of the control group was 2259 kg/m^3. For the experimental group, the unit weight of the F75-S and F75-M mixes with the addition of steel fiber was heavier (between 2338 and 2347 kg/m^3), while the unit weight of the F75-P mix only with the addition of polypropylene fiber was lighter (2270 kg/m^3).

3.2 Compressive strength

The measured compressive strength of each concrete mixture at 28 days of age was listed in Table 5, which was the average of three specimens. As can be seen from the table, the measured compressive strength was higher than the 28-day compressive strength required at room temperature. In addition, the compressive strength of the experimental group concrete incorporating steel fiber or polypropylene fiber was not significantly improved. This is because a relatively low fiber volume fraction was used in the designed concrete mixture. Moreover, even the addition of polypropylene fibers had a slight negative impact on the compressive strength of concrete.

It can be seen from Table 5 that the residual compressive strength of each group of concrete generally decreased with increasing temperature. However, when the temperature was 400℃, the residual compressive strength of the N75 and F75-P specimens increased instead. This is because of rapid drying of the concrete specimen (Siddique and Kaur

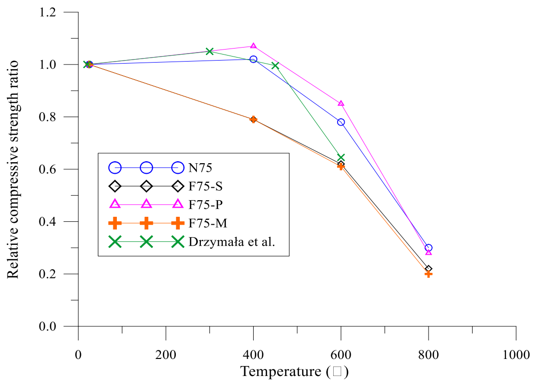

Fig. 3 Comparison of relative compressive strength ratio of concrete specimens

2012). Although the furnace temperature was maintained for an hour, the temperature inside the concrete was still lower than 400℃. Under the high temperature drying effect, the water vapor in the test specimen was evaded, which contributed to the improvement of strength. The test of Li and Bu (2011) also shows that the compressive strength of concrete after 200-300℃ was increased with the increase of temperature. In addition, the results of Drzymała *et al.* (2017) show that the compressive strength of fiber concrete after 300℃ was also higher than the initial value measured at 20℃. Deshpande *et al.* (2019) indicated that a slight increase in residual strength compared to room temperature strength may be associated with the favorable changes in the microstructure at high temperatures and the inherent variability of concrete material. Cheyrezy *et al.* (1995), Tai *et al.* (2011) have shown that high temperature could accelerate the pozzolanic reaction, increase the hydration product, reduce the diameter of the pores, and help to increase the compressive strength of concrete. But the residual compressive strength of each concrete mix decreased significantly after being exposed to 600℃. The reason is the strength loss was mainly caused by physical changes in the temperature range below 400℃. However, in the temperature range of 600-800℃, the attenuation of strength was mainly due to chemical degradation in hydrated products and aggregates, which was not directly related to the content and type of fibers (Deshpande *et al.* 2019). Especially, the residual compressive strength retained by the test specimens at 800℃ was about 20% to 30% of their respective compressive strength at room temperature. After exposure to high temperatures of 400, 600, and 800℃, the average residual compressive strength of the experimental group was 88%, 69%, and 23% of the room-temperature strength, respectively.

The relative compressive strength ratio was defined as the ratio of the strength after exposure to the target high temperature to the original strength at room temperature. The trend of this value versus temperature is shown in Fig. 3. The results of Drzymała *et al.* (2017) are also plotted in Fig. 3 for a comparison. As can be seen from the figure, the relative compressive strength ratio of the test results of Drzymała *et al.* was higher than 1 at a temperature range of 300 to 450℃. According to the test results in Fig. 3, the variation with temperature follows a similar trend for the F75-S and F75-M specimens. That is to say, the relative compressive strength ratios of the F75-S and F75-M specimens decreased rapidly with increasing temperature. By contrast, the relative compressive strength ratios of the F75-P specimens changed more slowly with increasing temperature. This is because the polypropylene fibers melted at high temperatures and created additional passages in this manner that helped to relieve internal vapor pressure and maintain a certain residual strength. From this result, the benefit of steel fibers to the residual compressive strength of concrete was limited. In contrast, polypropylene fibers can inhibit spalling after exposure to 400-600℃, thereby reducing internal flaws and effectively helping to maintain the residual strength of the concrete. This result is like the findings of Dong *et al.* (2008). However, as the temperature was further increased, the residual compressive strength ratios of each group of concrete significantly deteriorated; especially at a temperature of 800℃, the residual compressive strength ratios were below 0.30. After further inspection, it can be found that the residual compressive strength ratio of the concrete in the control group was slightly higher than that in the experimental group.

Table 6 Results of elastic modulus

Group	Mix No.	Elastic modulus (GPa)	Residual elastic modulus (GPa)		
		Room temperature	High temperature		
			400 ℃	600 ℃	800 ℃
Control group	N75	32.3	27.1	24.2	2.7
Experimental group	F75-S	31.6	26.4	15.5	6.5
	F75-P	37.3	25.0	23.1	2.0
	F75-M	38.6	30.6	13.3	6.8

3.3 Elastic modulus

The modulus of elasticity is defined by the slope of the linear region of the stress-strain curve. The results of the test for the elastic modulus of concrete specimens at 28 days of age are shown in Table 6. At room temperature, the elastic modulus of the F75-S specimen was a little less than that of the N75 specimen. But the magnitudes of the modulus of the F75-P and F75-M mixes were higher than that of the N75 specimen. On the whole, the residual elastic modulus of the concrete specimens decreased with increasing temperature in the fire test. In other words, exposure to high temperature resulted in a loss of elastic modulus in each group of concrete. As can be seen in Table 6, after exposure to different temperatures, the elastic modulus for the N75 specimens ranged from 2.7 to 27.1 GPa, while the elastic modulus for the F75-S, F75-P, and F75-M specimens ranged from 6.5 to 26.4 GPa, from 2.0 to 25.0 GPa, and from 6.8 to 30.6 GPa, respectively. At a temperature of 400℃, the residual elastic modulus of each concrete mix can be maintained at about 67-84% of the room-temperature value. With a further increase in temperature to 600℃, the residual elastic modulus of each concrete mix can still maintain about 34-75% of the room-temperature value. For concrete with polypropylene fibers,

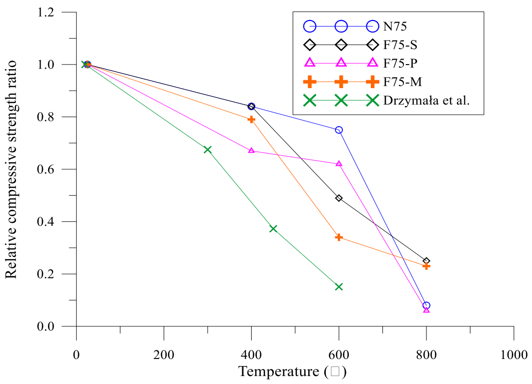

Fig. 4 Comparison of elastic modulus of concrete specimens

when temperature ranged at 400-600℃, the loss of elastic modulus was not significant. But after exposure to 800℃, the residual elastic modulus of the F75-P specimens was only 6% of the original value, while the residual elastic modulus of the F75-S and F75-M specimens was still 25% and 23% of the original value, respectively. The decrease in the elastic modulus of concrete exposed to high temperatures is mainly due to the increase in the volume of the porous and the cracking of the interface zone between the paste and the aggregate.

Moreover, the relative elastic modulus ratio versus temperature curves for each group of concrete are shown in Fig. 4. The results of Drzymała *et al.* (2017) are also plotted in Fig. 4 for a comparison. From Fig. 4, it can be seen that the relative elastic modulus ratio was a function of the mixture proportions and exposure temperature. After exposure to 400℃, the relative elastic modulus ratio of all the mixtures dropped sharply. This is due to the combined effect of mechanical degradation and chemical degradation. In addition, the variation of the relative elastic modulus ratio for the F75-S specimen was quite similar to that of the F75-M specimen. It is worth noting that as the temperature rose, the decreasing trend of the relative elastic modulus ratio was obviously more serious than the decreasing trend of the compressive strength. This is because the elastic modulus is more sensitive to cracks at the macroscopic or microscopic scale induced by high temperatures (Hsu *et al.* 1963).

On the other hand, the stress-strain curves of the F75-S and F75-M specimens are shown in Fig. 5. It can be seen from Fig. 5 that the stress-strain curves of the F75-S and F75-M specimens were similar after 400-800℃. The initial slope of ascending branches of the stress-strain curves showed a linear relationship before exposure to high temperatures, and its slope was quite steep. However, after exposure to high temperatures, the stress-strain curves of some specimens at the beginning of loading exhibit atypical nonlinearities, also known as a concave-up curve. This result is consistent with Chang *et al.* (2006), Tai *et al.* (2011). The reason for this is that during this pre-elastic hardening, the concrete stiffened as it approached the linear elastic region (Way and Wille 2016). Chang *et al.* (2016) believe that the closing of pre-existing cracks from heating and cooling can cause this behavior. The matrix shrinkage

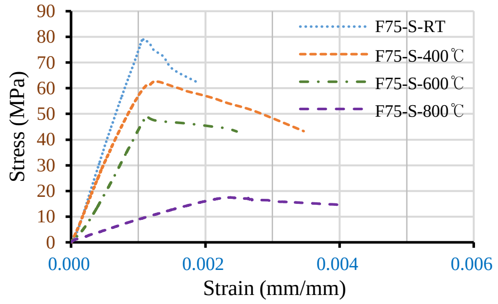

(a) Experimental group F75-S

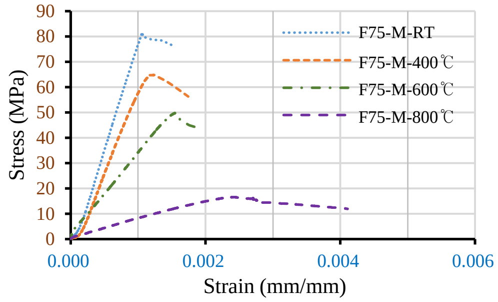

(b) Experimental group F75-M

Fig. 5 Stress versus strain curve of concrete specimens

Table 7 Results of flexural strength

Group	Mix No.	Flexural strength (MPa)	Residual flexural strength (MPa)		
		Room temperature	High temperature		
			400 ℃	600 ℃	800 ℃
Control group	N75	7.4	7.7	5.1	1.7
Experimental group	F75-S	7.9	11.4	5.8	2.0
	F75-P	6.7	9.5	5.9	1.1
	F75-M	7.5	9.9	5.7	1.5

caused by dehydration of calcium hydroxide, thermal incompatibility between aggregates and cement paste, and the expansion of steel fiber are factors that cause cracking (Zheng *et al.* 2012). On the whole, the initial slope of ascending branches decreased with increasing temperature. This is attributed to the decomposition and dehydration of the hydrated product at high temperatures and cracks caused by pore pressure. In addition, the descending slope after the peak stress was influenced by the mixture proportions of the specimen and exposure temperatures. As the exposure temperature increased, the curve gradually became flatter and more extended until the concrete specimens crushed. In other words, although the ductility of the test piece increased with increasing temperature, the peak stress rapidly decreased.

3.4 FLexural strength

The results of the test for the flexural strength (i.e., modulus of rupture) of concrete specimens at 28 days of age are shown in Table 7. At room temperature, the flexural strength of the F75-P specimens was a little less than that of the N75 specimens. But the flexural strength of the F75-S and F75-M specimens were higher than that of the N75 specimen. This is due to the bridging effect of the fibers, the flexural strength of the concrete increases, and the fracture behavior of the concrete becomes more ductile. After exposure to different high temperatures, although thermal energy generated by high temperature caused cracks to form between the cement paste and fibers, the fibers could prevent crack propagation and help to strengthen the specimen to some extent. As can be seen in Table 7, after exposure to 200-800℃, the residual flexural strength of the N75 specimens ranged from 1.7 to 7.7 MPa, while the residual flexural strength for the F75-S, F75-P, and F75-M specimens ranged from 2.0 to 11.4 MPa, from 1.1 to 9.5 MPa, and from 1.5 to 9.9 MPa, respectively. At a temperature of 400℃, the concrete specimens reached peak strength. This is because the temperature inside the test specimen was still lower than 400℃ although the furnace temperature was maintained for 60 minutes. In other words, the average temperature of the test specimen had not yet reached 400℃. Owing to the rapid drying of the specimen exposed to high temperature, the moisture in matrix pores can be easily evaporated (Siddique and Kaur 2012). As a result, the residual flexural strength increased due to the effect of high-temperature drying. However, after being exposed to 600℃ for 60 minutes, the residual flexural strength of each concrete mix decreased significantly. Especially, after exposure to 800℃, the residual flexural strength of the F75-P specimens was 16% of the original value; while the residual flexural strength of the F75-S and F75-M specimens was 25% and 20% of the original value, respectively.

Moreover, the relative flexural strength ratio versus temperature curves for each group of concrete are shown in Fig. 6. From Fig. 6, when the temperature was 600℃, the residual flexural strength ratios of the concrete specimens decreased significantly; among them, the residual flexural strength ratios of the experimental group were higher than 0.7, while the residual flexural strength ratio of the control group was lower than 0.7. Overall, the addition of fiber mitigated to a certain degree the degradation in flexural strength of HSC after exposure to high temperatures.

The load versus midspan deflection curves for each group of concrete specimens are shown in Fig. 7. As can be seen from Fig. 7, in most cases, the load-displacement curve was linear in the region before the peak point. In addition,

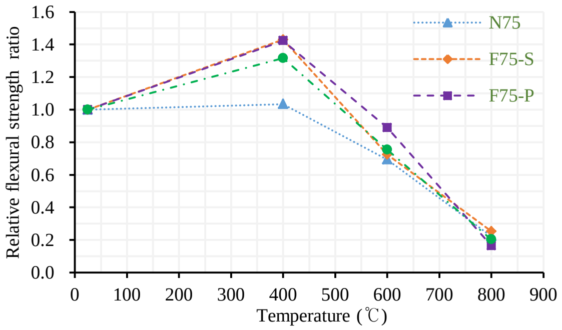

Fig. 6 Comparison of the relative flexural strength ratio of concrete specimens

the influence of adding fiber was the mechanical benefit which ensued from the ability of the fiber to bridge the cracks. Therefore, all test specimens of the experimental group incorporating fiber showed greater loads and displacement capabilities than the control group. In particular, test specimens incorporating steel fibers exhibited a better displacement capacity. When the temperature was 400℃, regardless of the control group or the experimental group, the slope of the initial slope of ascending branches of the load versus midspan deflection curves was greater than the slope at room temperature. The ultimate flexural load of the control group N75 increased only slightly, while the ultimate flexural load of the experimental group (F75-S, F75-P, and F75-M) increased significantly. The reason for this is as described previously, mainly due to the effect of high-temperature drying, which increased its strength and, in turn, increased the flexural load of the test specimen (Siddique and Kaur 2012). It is also worth noting that the increase in the ultimate flexural load of the N75 specimen was minimal. In addition, when the temperature was 600℃, the slope of the ascending branches of the load versus midspan deflection curves reduced regardless of the control group or the experimental group, but there was no case of rapid decay. However, when the temperature was 800℃, the slopes of ascending branches of the load versus midspan deflection curves of the control and experimental groups significantly reduced. Regarding the descending branches of the load versus midspan deflection curves, the rate of decline in the flexural load of the test specimens at the room temperature or at high temperatures was more moderate in the F75-S and F75-M specimens with steel fibers. This indicates that the F75-P specimen, which used polypropylene fibers alone, did not provide excellent strength and ductility at low to medium temperatures, but steel fibers provided fiber bridging at higher temperatures, allowing the F75-S and F75-M specimens to retain a significant proportion of their flexural strength and ductility. In other words, the post-peak behavior at higher temperatures is mainly affected by steel fibers rather than by polypropylene fibers.

On the other hand, in order to further understand the differences between the control group and the experimental group, the load versus midspan deflection curves at room temperature and at various fire temperature were analyzed. At room temperature and at different elevated heating temperatures, the toughness (i.e., the area under the load versus deflection curve up to fracture) of the control group was relatively lower than that of the experimental group. In addition, Fig. 8 shows that the load-deflection curves of the F75-S and F75-M specimens were both more ductile at room temperature or at various fire temperatures. From Fig. 8, the presence of fibers increased the toughness of the experimental group. Moreover, the load versus midspan deflection curves of the F75-S and F75-M specimens showed two peak points; the first peak was the ultimate flexural load; the second peak was due to the load provided by the steel fibers after the cracks were formed. The failure deflection of the N75 and F75-P specimens was quite close to the crack deflection at room temperature or at various fire temperatures. At room temperature, the bridging effect of polypropylene fibers made the flexural strength and

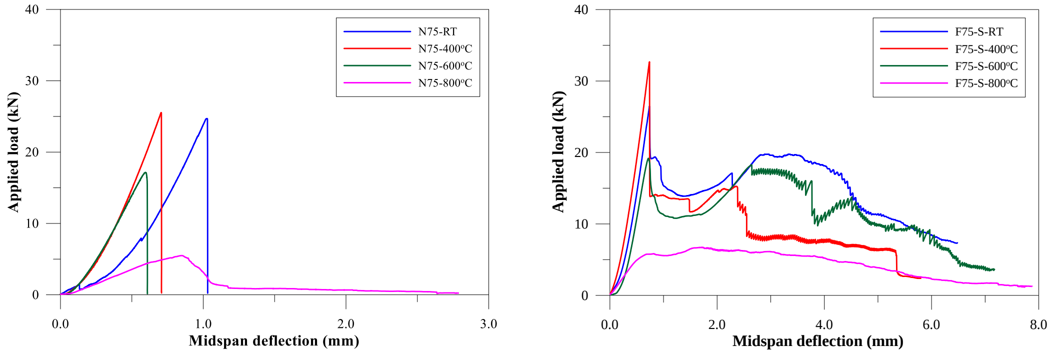

(a) Control group N75 (b) Experimental group F75-S

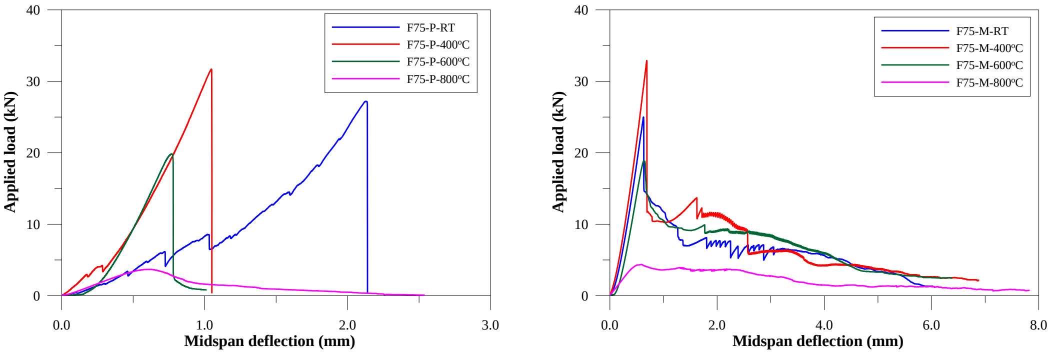

(c) Experimental group F75-P (d) Experimental group F75-M

Fig. 7 Load-deflection curves of concrete specimens before and after high temperatures

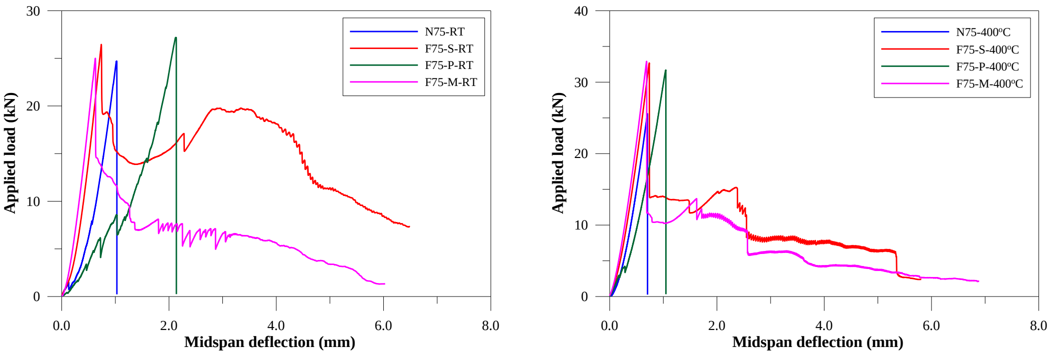

(a) Room temperature (b) Fire temperature 400℃

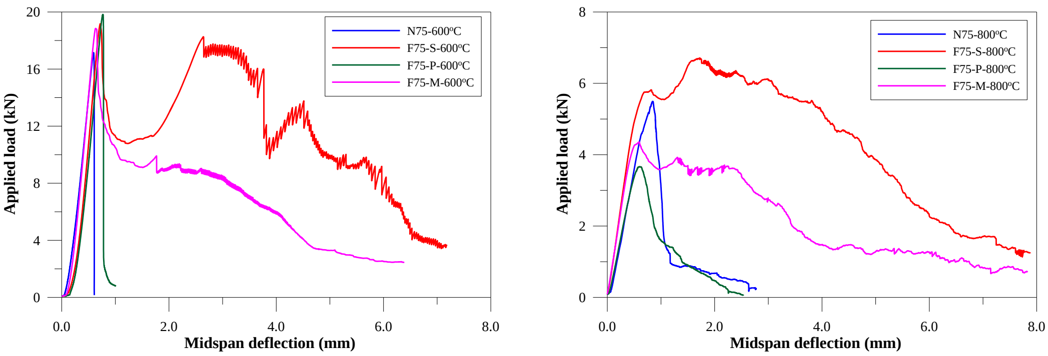

(c) Fire temperature 600℃ (d) Fire temperature 800℃

Fig. 8 Comparison of the load-deflection curves of concrete specimens before and after high temperatures

ductility of the F75-P specimen better than that of the N75 specimen. However, at higher temperatures, the melting of the polypropylene fibers led to complete loss of fiber bridging, resulting in a brittle failure behavior. In contrast, as can be seen from Fig. 8, the specimen containing steel fibers exhibited strain hardening behavior. Therefore, the F75-S and F75-M specimens could achieve a failure deflection of more than 6 times the crack deflection, indicating that the load-deflection curve was more ductile. In other words, the post-peak region of the specimen containing steel fibers had a better toughness. Overall, the load versus midspan deflection curves of the N75 and F75-P specimens were similar, while the load versus midspan deflection curves of the F75-S and F75-M specimens were similar, and both had a better flexural toughness.

4. Conclusions

In this study, the effects of individual and hybrid fiber on the residual mechanical properties of high-strength fiber reinforced concrete were investigated after exposure to 400-800℃ in addition to the room temperature. On the basis of the above experimental results and discussion, the following conclusions were drawn:

- The benefit of steel fibers on the residual compressive strength of concrete was limited. In contrast, polypropylene fibers can inhibit spalling after exposure to 400-600℃, thereby reducing internal cracks and helping to maintain the residual compressive strength and flexural strength of the concrete.
- High-strength fiber reinforced concrete lost its modulus of elasticity much faster than its compressive strength when exposed to high temperatures.
- After exposure to 800℃, the flexural load of each series of concrete decreased rapidly, and its residual flexural load ratio was less than 0.25.
- Both at room temperature or elevated temperatures, the load-deflection curve of fiber reinforced concrete had a better fracture toughness. Especially, the typical load-deflection response of the steel fiber reinforced specimen showed a double peak, indicating that its toughness was better.

Acknowledgments

This work was supported by the Ministry of Science and Technology (MOST), Taiwan. The author expresses his gratitude and sincere appreciation to MOST for financing this research work.

References

ASTM C150/C150M-15 (2015), Standard Specification for Portland Cement, ASTM International, West Conshohocken, PA.

ASTM C33/C33M-13 (2013), Standard Specification for Concrete Aggregates, ASTM International, West Conshohocken, PA.

ASTM C469/C469M-14 (2014), Standard Test Method for Static Modulus of Elasticity and Poisson's Ratio of Concrete in Compression, ASTM International, West Conshohocken, PA.

ASTM C78/C78M-18 (2018), Standard Test Method for Flexural Strength of Concrete (Using Simple Beam with Third-Point Loading), ASTM International, West Conshohocken, PA.

Bastos, G., Patiño-Barbeito, F., Patiño-Cambeiro, F. and Armesto, J. (2016), "Admixtures in cement-matrix composites for mechanical reinforcement, sustainability, and smart Features", *Mater.*, **9**, 972. https://doi.org/10.3390/ma9120972.

Bilodeau, A., Kodur, V.K.R. and Hoff, G.C. (2004), "Optimization of the type and amount of polypropylene fibres for preventing the spalling of lightweight concrete subjected to hydrocarbon fire", *Cement Concrete Compos.*, **26**, 163-174. https://doi.org/10.1016/S0958-9465(03)00085-4.

Chan, Y.N., Luo, X. and Sun, W. (2000), "Compressive strength and pore structure of high-performance concrete after exposure to high temperature up to 800℃", *Cement Concrete Res.*, **30**, 247-251. https://doi.org/10.1016/S0008-8846(99)00240-9.

Chang, Y.F., Cheng, Y.H., Sheu, M.S. and Yao, G.C. (2006), "Residual stress-strain relationship for concrete after exposure at high temperatures", *Cement Concrete Res.*, **36**(10), 1999-2005. https://doi.org/10.1016/j.cemconres.2006.05.029.

Cheyrezy, M., Maret, V. and Frouin, L. (1995), "Microstructural analysis of RPC (reactive powder concrete)", *Cement Concrete Res.*, **25**(7), 1491-1500. https://doi.org/10.1016/0008-8846(95)00143-Z.

Deshpande, A.A. and Kumar, D.R. (2019), "Influence of high temperatures on the residual mechanical properties of a hybrid fiber-reinforced strain-hardening cementitious composite", *Constr. Build. Mater.*, **208**, 283-295. https://doi.org/10.1016/j.conbuildmat.2019.02.129.

Ding, Y., Azevedo, C., Aguiar, J.B. and Jalali, S. (2012), "Study on residual behaviour and flexural toughness of fibre cocktail reinforced self compacting high performance concrete after exposure to high temperature", *Constr. Build. Mater.*, **26**, 21-31. https://doi.org/10.1016/j.conbuildmat.2011.04.058.

Dong, X., Ding, Y. and Wang, T.J. (2008), "Spalling and mechanical properties of fiber reinforced high-performance concrete subjected to fire", *Wuhan Univ. Technol.-Mater. Sci. Ed.*, **23**(5), 743-749. https://doi.org/10.1007/s11595-007-5743-5.

Drzymała, T., Jackiewicz-Rek, W., Tomaszewski, M., Kuś, A., Gałaj, J. and Šukys, R. (2017), "Effects of high temperature on the properties of High Performance Concrete (HPC)", *Procedia Eng.*, **172**, 256-263. https://doi.org/10.1016/j.proeng.2017.02.108.

Hsu, T.T.C., Slate, F.O., Sturman, G.M. and Winter, G. (1963), "Microcracking of plain concrete and the shape of the stress-strain curve", *ACI Mater. J.*, **60**(2), 209-224.

Khaliq, W. and Kodur, V. (2011), "Thermal and mechanical properties of fiber reinforced high performance self-consolidating concrete at elevated temperatures", *Cement Concrete Res.*, **41**, 1112-1122. https://doi.org/10.1016/j.cemconres.2011.06.012.

Kim, N.W., Lee, H.H. and Kim, C.H. (2016), "Fracture behavior of hybrid fiber reinforced concrete according to the evaluation of crack resistance and thermal", *Comput. Concrete*, **18**(5), 685-96.

Ko, J., Ryu, D. and Noguchi, T. (2011), "The spalling mechanism of high-strength concrete under fire", *Mag. Concrete Res.*, **63**(5), 357-370. http://dx.doi.org/10.1680/macr.10.00002.

Kodur, V. (2014), "Properties of concrete at elevated temperatures", ISRN Civil Engineering Volume, Article ID 468510.

Larrard, F. and Sedran, T. (2002), "Mixture proportioning of high performance concrete", *Cement Concrete Res.*, **32**(11), 1699-1704. https://doi.org/10.1016/S0008-8846(02)00861-X.

Lee, H.H. and Yi, S.T. (2016), "Structural performance evaluation of steel fiber reinforced concrete beams with recycled aggregates", *Comput. Concrete*, **18**(5), 741-756. https://doi.org/10.4334/JKCI.2015.27.3.215.

Li, X. and Bu, F. (2011), "Residual Strength for Concrete after Exposure to High Temperatures"Ed. Dai, M., *Innovative Computing and Information. ICCIC 2011, Communications in Computer and Information Science*, **232**, Springer, Berlin, Heidelberg.

Mehta, P.K. and Monteiro, P.J.M. (2006), *Concrete: Microstructure, Properties, and Materials*, 3rd Edition, The McGraw-Hill Companies, Inc., New York.

Nematzadeh, M. and Poorhosein, R. (2017), "Estimating properties of reactive powder concrete containing hybrid fibers using UPV", *Comput. Concrete*, **20**(4), 491-502. https://doi.org/10.12989/cac.2017.20.4.491.
Ozawa, M. and Morimoto, M. (2014), "Effects of various fibres on high-temperature spalling in high-performance concrete", *Constr. Build. Mater.*, **71**, 83-92. https://doi.org/10.1016/j.conbuildmat.2014.07.068.
Poon, C.S., Shui, Z.H. and Lam, L. (2004), "Compressive behavior of fiber reinforced high-performance concrete subjected to elevated temperatures", *Cement Concrete Res.*, **34**, 2215-2222. https://doi.org/10.1016/j.cemconres.2004.02.011.
Qadi, A.A.N.S. and Sleiman, M.A. (2014), "Effect of fibre content and specimen shape on residual strength of polypropylene fibre self-compacting concrete exposed to elevated temperatures", *J. King Saud Univ.–Eng. Sci.*, **26**, 33-39. https://doi.org/10.1016/j.jksues.2012.12.002.
Saleem, M. (2017), "Study to detect bond degradation in reinforced concrete beams using ultrasonic pulse velocity test method", *Struct. Eng. Mech.*, **64**(4), 427-436. https://doi.org/10.12989/sem.2017.64.4.427.
Sanjayan, G. and Stocks, L.J. (1993), "Spalling of high-strength silica fume concrete in fire", *ACI Mater. J.*, **90**(2), 170-173.
Serrano, R., Cobo, A., Prieto, M.I. and González, M.D.N. (2016), "Analysis of fire resistance of concrete with polypropylene or steel fibers", *Constr. Build. Mater.*, **122**, 302-309. https://doi.org/10.1016/j.conbuildmat.2016.06.055.
Siddique, R. and Kaur, D. (2012), "Properties of concrete containing ground granulated blast furnace slag (GGBFS) at elevated temperatures", *J. Adv. Res.*, **3**, 45-51. https://doi.org/10.1016/j.jare.2011.03.004.
Sideris, K.K. and Manita, P. (2013), "Residual mechanical characteristics and spalling resistance of fiber reinforced self-compacting concretes exposed to elevated temperatures", *Constr. Build. Mater.*, **41**, 296-302. https://doi.org/10.1016/j.conbuildmat.2012.11.093.
Sideris, K.K., Manita, P. and Chaniotakis, E. (2009), "Performance of thermally damaged fibre reinforced concretes", *Constr. Build. Mater.*, **23**, 1232-1239. https://doi.org/10.1016/j.conbuildmat.2008.08.009.
Somayaji, S. (2001), *Civil Engineering Materials*, Prentice Hall, Upper Siddle River, New Jersey.
Tai, Y.S., Pan, H.H. and Kung, Y.N. (2011), "Mechanical properties of steel fiber reinforced reactive powder concrete following exposure to high temperature reaching 800°C", *Nucl. Eng. Des.*, **241**, 2416-2424. https://doi.org/10.1016/j.nucengdes.2011.04.008.
Varona, F.B., Baeza, F.J., Bru, D. and Ivorra, S. (2018), "Influence of high temperature on the mechanical properties of hybrid fibre reinforced normal and high strength concrete", *Constr. Build. Mater.*, **159**, 73-82. https://doi.org/10.1016/j.conbuildmat.2017.10.129.
Way, R. and Wille, K. (2016), "Effect of heat-induced chemical degradation on the residual mechanical properties of ultrahigh-performance fiber-reinforced concrete", *J. Mater. Civil Eng.*, **28**(4), 04015164. https://doi.org/10.1061/(ASCE)MT.1943-5533.0001402.
Xiong, M.X. and Richard Liew, J.Y. (2015), "Spalling behavior and residual resistance of fibre reinforced Ultra-High performance concrete after exposure to high temperatures", *Materiales de Construccion*, **65**(320), 71.
Xu, M., Hallinan, B. and Wille, K. (2016), "Effect of loading rates on pullout behavior of high strength steel fibers embedded in ultra-high performance concrete", *Cement Concrete Compos.*, **70**, 98-109.
Yan, Z., Shen, Y., Zhu, H., Li, X. and Lu, Y. (2015), "Experimental investigation of reinforced concrete and hybrid fibre reinforced concrete shield tunnel segments subjected to elevated temperature", *Fire Saf. J.*, **71**, 86-99. https://doi.org/10.1016/j.firesaf.2014.11.009.
Zhang, C., Li, Z. and Ding, Y. (2018), "Effect of hybrid fibers on flexural performance of reinforced SCC symmetric inclination beams", *Comput. Concrete*, **22**(2), 209-230. https://doi.org/10.12989/cac.2018.22.2.209.
Zheng, W., Li, H. and Wang, Y. (2012), "Compressive behaviour of hybrid fiber-reinforced reactive powder concrete after high temperature", *Mater. Des.*, **41**, 403-409. https://doi.org/10.1016/j.matdes.2012.05.026.

CC